Week 5

1 Nuclear energy generation

During most of their lifetimes, stars derive the energy that they radiate from nuclear reactions. The gradual change in chemical composition as the reactions proceed determines the evolution of stars. Hence, to follow the life history of a star, it is important to understand the properties of the nuclear reactions.

Nuclear processes in stars involve fusion of nuclei to build heavier nuclei, and at the end stages of stellar evolution fission processes may also become important. During these processes, key physical quantities are conserved:

- The baryon number - the number of protons, neutrons and their anti-particles
- The lepton number - the numbers of electrons and neutrinos and their anti-particles
- Total charge
- Total mass-energy

According to Einstein's mass-energy relationship, a nuclear reaction in which the total mass of the final products is smaller than that of the initial reacting nuclei is exothermic, that is it releases an amount of energy

$$Q = \left(\sum_i m_i - \sum_f m_f \right) c^2, \tag{1}$$

where m represents the mass and c is the speed of light. The mass, m, of a nucleus with atomic number Z and mass number A differs from the sum of the masses of the Z protons and $(A - Z)$ neutrons, which build up the nucleus, by the quantity

$$\Delta m = Z m_{\rm p} + (A - Z) m_{\rm n} - m, \tag{2}$$

where the total binding energy is given by

$$B = \Delta m c^2. \tag{3}$$

In order to dissociate the nucleus into its component neutrons and protons, one needs to supply an amount of energy $B = \Delta m c^2$.

A useful quantity to consider is the binding energy per nucleon, B/A, for a nucleus. This quantity is plotted in Fig. 1, and shows that there is a sharp rise for $A > 1$, followed by a broad maximum of 8.7 MeV around $A = 56$, with a shallow drop-off for $A > 60$. Fusion reactions are expected to proceed when the total amount of binding energy associated with the reaction products exceeds that associated with the reactants. As indicated by the diagram, it is very energetically favourable to fuse hydrogen nuclei to form ^{4}He. It remains energetically favourable to fuse elements up to ^{56}Fe, which sits at the peak of the energy per nucleon figure. It becomes energetically unfavourable for fission reactions to occur for heavier nuclei. For example, nuclear reactions that fuse 112 nucleons to form a pair of ^{56}Fe nuclei will release at total of $\approx 2 \times 56 \times 8.7$ MeV of binding energy ($= 974.4$ MeV). Combining two ^{56}Fe nuclei to form a ^{112}Ca (Cadmium) nucleus will release a total of $\approx 112 \times 8$ ($= 896$ MeV), which is smaller than the binding energy associated with the two ^{56}Fe nuclei. Hence, at the end stages of

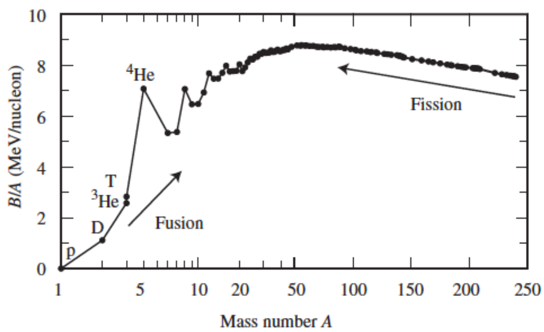

Figure 1: Binding energy per nucleon

stellar evolution the reactions that build elements heavier that Fe and Ni are endothermic rather than exothermic as they require the input of energy to proceed. As will be discussed in a future lecture, this explains why iron and nickel are abundant elements in the Solar System: they are the end products of nucleosynthesis in massive stars.

1.1 The Coulomb barrier

In order for a fusion reaction to occur, two nuclei need to approach one another and collide such that the distance of closest approach equals the sum of the sizes of the nuclei, as it is at these distances that the strong nuclear force can operate to bind the nuclei together. The radius of a hydrogen nucleus (proton) is $r_{\rm p} \approx 10^{-15}$ m. As the two nuclei approach one another, however, they are repelled by the electrostatic Coulomb force which forms a potential barrier that must be overcome to allow the nuclei to touch. This potential barrier is illustrated by the upper image in Fig. 2. We can estimate the size of the potential barrier, and hence the amount of kinetic energy that the nuclei need to have in order to overcome it, by calculating the work that needs to be done in bringing two nuclei from infinity to within touching distance

$$W = \int_{\infty}^{(r_1+r_2)} \mathbf{F}\cdot d\mathbf{r} = \int_{\infty}^{(r_1+r_2)} \frac{Z_1 Z_2 e^2}{4\pi\epsilon_0 r^2} dr = \frac{Z_1 Z_2 e^2}{4\pi\epsilon_0 (r_1+r_2)} \quad (4)$$

where $\epsilon_0 = 8.85 \times 10^{-12}$ m^{-3} kg^{-1} s^4 A^2 is the permittivity of free space. From lecture 2, we know that the average kinetic energy of the nuclei in a plasma of temperature T is $\langle U \rangle = (3k_{\rm B}T)/2$, hence we can estimate the temperature at which the Coulomb barrier can be overcome during a typical collision by setting $\langle U \rangle = W$, giving

$$T = \frac{Z_1 Z_2 e^2}{6\pi\epsilon_0 k_{\rm B}(r_1+r_2)}. \quad (5)$$

This gives an estimate of $T = 10^{10}$ K, which is obviously much higher than the value of $T = 1.5 \times 10^7$ K that is estimated for the centre of the Sun. We should also consider the particles in the Maxwell-Boltzmann distribution that have higher energies than the average, as these may be able to overcome the Coulomb barrier. The probability of having an energy between E_1 and E_2 in a plasma of temperature T is given by

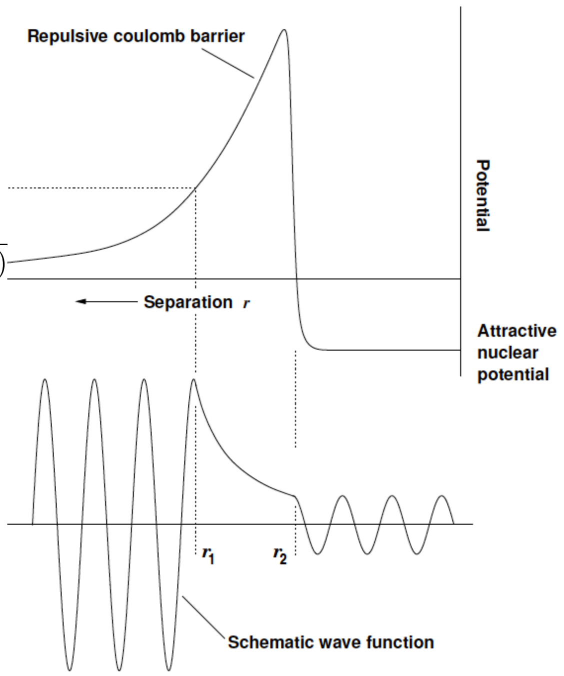

Figure 2: Top image shows schematic diagram of Coulomb barrier and the attractive strong force. Bottom image shows exponentially decreasing amplitude of wavefunction as nuclei tunnel through Coulomb barrier.

$$\int_{E_1}^{E_2} f(E)dE = \int_{E_1}^{E_2} 2\sqrt{\frac{E}{\pi}} \left(\frac{1}{k_{\rm B}T}\right)^{3/2} \exp\left(-\frac{E}{k_{\rm B}T}\right) dE. \quad (6)$$

Approximating the integrand as a constant centred on the energy associated with the Coulomb barrier derived above (which we denote as $E_{\rm C}$), we can make a simple estimate of the probability of finding particles with energies in range $E_{\rm C} - E_{\rm C}/2 \le E \le 2E_{\rm C} + E_{\rm C}/2$ where $E_{\rm C}$ corresponds to the Coulomb barrier energy

$$2\sqrt{\frac{E_{\rm C}}{\pi}} \left(\frac{1}{k_{\rm B}T}\right)^{3/2} \exp\left(-\frac{E_{\rm C}}{k_{\rm B}T}\right) \int_{E_{\rm C-E_C/2}}^{E_{\rm C}+E_{\rm C}/2} dE = 2\sqrt{\frac{E_{\rm C}}{\pi}} \left(\frac{1}{k_{\rm B}T}\right)^{3/2} \exp\left(-\frac{E_{\rm C}}{k_{\rm B}T}\right) E_{\rm C} \quad (7)$$

For a temperature of $T = 1.5 \times 10^7$ K this gives a probability $P(E_{\rm C}) = 5 \times 10^4 \times \exp(-1000)$. Such a small probability indicates that there are insufficient particles in the high energy tail of the Maxwell-Boltzmann distribution to explain the energy output of the Sun.

1.2 Quantum tunnelling

The solution to the problem of overcoming the Coulomb barrier can be found in quantum mechanics, and was originally elucidated by George Gamow. Heisenberg's uncertainty principle states that there is a fundamental uncertainty in defining both the position and momentum of two nuclei as they collide, and hence at the moment of closest approach the two nuclei may be closer together than permitted by classical physics such that they have crossed the Coulomb barrier and are close enough to be bound by the strong force. This process is known as quantum tunnelling, and heuristically the probability of it occurring scales as $\exp(-r_0/\lambda)$, where r_0/λ is the ratio of the classical turning point, r_0, to the de Broglie wavelength of the particles, $\lambda = h/p$, where p is the particle momentum and h is Planck's constant. The idea here is that quantum tunnelling becomes more probable when the distance of closest approach between the nuclei becomes comparable to or smaller than the de Boglie wavelength. The temperature, $T_{\rm tunnel}$, at which the average particle collision has $\lambda \approx r_0$ can be estimated by combining the Coulomb energy

$$E = \frac{Z_1 Z_2 e^2}{4\pi\epsilon_0 r_0} \tag{8}$$

with the mean thermal energy of a gas a temperature T

$$E = \frac{3}{2} k_{\rm B} T$$

and the de Broglie wavelength

$$\lambda = \frac{h}{p}$$

and the relation between energy and momentum

$$E = \frac{p^2}{2m},$$

giving the expression

$$T_{\rm tunnel} = \frac{4m_{\rm H}}{3k_{\rm B}h^2}\left(\frac{Z_1 Z_2 e^2}{4\pi\epsilon_0}\right)^2. \tag{9}$$

Note that equation (9) is obtained by substituting $r_0 \to \lambda$ in equation (8) and solving for the temperature. For hydrogen nuclei, we find that $T_{\rm tunnel} \approx 2 \times 10^7$ K, indicating that tunnelling will have a sufficient probability of occurring at the centre of the Sun to explain the observed energy output.

1.3 Nuclear reaction rates and energy release

We now consider the rate at which nuclear reactions occur between two types of nuclei, A and B, and introduce the concept of the reaction cross section, $\sigma(v)$. This has the units of length^2, and is related to the probability that a reaction will occur as a nucleus of type A approaches a nucleus of type B with collision velocity v.

Using a simple geometrical argument, and working in a frame in which a nucleus of type A moves relative to nuclei of type B with velocity v, we can see that the volume swept out per unit time by a nucleus of type A is given

$$V_A = \sigma(v)v. \tag{10}$$

The number of reactions that the nucleus of type A can experience is then

$$N_{\rm R} = n(B)\sigma(v)v, \tag{11}$$

where $n(B)$ is the number of nuclei of type B per unit volume. The number of reactions per unit volume per unit time is then

$$R(v) = n(A)n(B)\sigma(v)v, \tag{12}$$

where $n(A)$ is the number of nuclei of type A per unit volume. Note $R(v)$ is the reaction rate per unit volume for the specific value of velocity v. We need to integrate over the velocity to get the total reaction rate

$$R = n(A)n(B)\int_0^\infty v\sigma(v)f(v)dv \equiv n(A)n(B)\langle\sigma(v)v\rangle \quad \left[\mathrm{m}^{-3}\,\mathrm{s}^{-1}\right] \tag{13}$$

where $f(v)$ is the Maxwellian velocity distribution, and the angle brackets denote a weighted average.

We now need to consider what form to expect for $\langle\sigma(v)v\rangle$. We expect the fusion cross-section $\sigma(v)$ to be proportional to the target area seen by the reacting nuclei, which is given by to $\pi\lambda^2$, where λ is the de Broglie wavelength. We note that $\lambda^2 \propto 1/E$, where E is the kinetic energy of the particles. We also expect the fusion cross-section to depend on the details of the nuclear physics, which we encapsulate through the factor $S(E)$, noting that this is obtained experimentally. Finally, the probability of a reaction occurring must be proportional to the probability of quantum tunnelling. This is obtained by solving the Schroedinger equation for the potential shown in Fig. 2, and noting that the probability of finding a pair of nuclei with a given separation, d, is proportional to $|\psi(d)|^2$, where ψ is the wave function (see discussion in Chapter 4 of The Physics of Stars by A.C. Philips). The resulting probability of tunnelling is given by

$$P(E) = \exp\left(-\sqrt{\frac{E_\mathrm{G}}{E}}\right),$$

where E_G is the Gamow energy

$$E_\mathrm{G} = 2m_\mathrm{R}c^2(\pi\alpha Z_1 Z_2)^2 \quad (= 493\,\mathrm{keV}\ \text{for proton} - \text{proton fusion})$$

where $m_\mathrm{R} = m_A m_B/(m_A + m_B)$ is the reduced mass and α is the fine structure constant

$$\alpha = \frac{e^2}{4\pi\epsilon_0\hbar c} \simeq \frac{1}{137}.$$

Note: For two colliding nuclei, the energy available for overcoming the potential barrier is given by the relative kinetic energy

$$U = \frac{1}{2}m_\mathrm{r}v_{12}^2 \tag{14}$$

where m_r is the reduced mass, defined by $m_\mathrm{r} = m_1 m_2/(m_1 + m_2)$, and $v_{12} = |\mathbf{v}_1 - \mathbf{v}_2|$ is the magnitude of the relative velocity. For a Maxwellian distribution we can write $v = v_{12}$.

Collecting terms we can write

$$\sigma(E) = \frac{S(E)}{E}\exp\left(-\sqrt{\frac{E_\mathrm{G}}{E}}\right) \tag{15}$$

In a Maxwellian distribution, the probability that a particle will have energy E at kinetic temperature T is given by

$$f(E)dE = \frac{2}{\sqrt{\pi}}\left(\frac{E}{k_\mathrm{B}T}\right)\exp\left(-\frac{E}{k_\mathrm{B}T}\right)\frac{dE}{(k_\mathrm{B}TE)^{1/2}} \tag{16}$$

Noting that $v = \sqrt{2E/m_\mathrm{R}}$, we can write

$$\langle\sigma(v)v\rangle = \int_0^\infty \frac{S(E)}{E}\exp\left(-\sqrt{\frac{E_\mathrm{G}}{E}}\right)\sqrt{\frac{2E}{m_\mathrm{R}}}\frac{2}{\sqrt{\pi}}\left(\frac{E}{k_\mathrm{B}T}\right)\exp\left(-\frac{E}{k_\mathrm{B}T}\right)\frac{dE}{(k_\mathrm{B}TE)^{1/2}} \tag{17}$$

which can be simplified to read

$$\langle\sigma(v)v\rangle = \left(\frac{8}{\pi m_\mathrm{R}}\right)^{1/2}\frac{1}{(k_\mathrm{B}T)^{3/2}}\int_0^\infty S(E)\exp\left(-\sqrt{\frac{E_\mathrm{G}}{E}}\right)\exp\left(-\frac{E}{k_\mathrm{B}T}\right)dE. \tag{18}$$

Note that this applies to some fixed temperature, T. The nuclear reaction rate can clearly be seen to depend on two competing factors: the exponentially decreasing probability of particles having energies higher than $\approx k_{\mathrm{B}}T$ in a Maxwellian distribution, and the increasing probability of quantum tunnelling occurring as E increases towards E_{G}. As illustrated by Fig. 3, the integrand in eqn. (18) in peaked around a specific range of energies that correspond to those at which most of the nuclear reactions take place. This is known as the Gamow Peak.

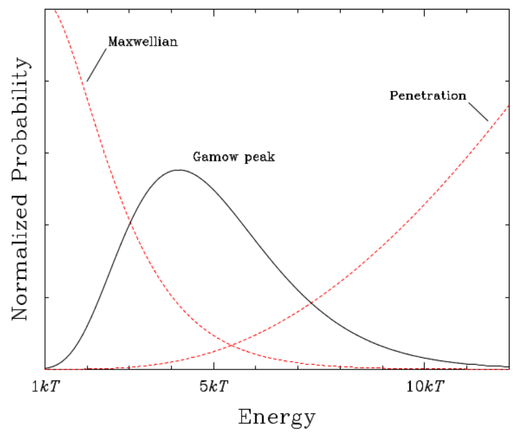

Figure 3: This figure illustrates the competing influences of the decreasing probability of having high energy particles in the Maxwell distribution, and the increasing probability of tunnelling at high energies, giving rise to the Gamow peak.

The amount of energy released per reaction is denoted by Q, as discussed above. Hence the rate of energy generation per unit volume is given by

$$\frac{dU}{dt} = n(A)n(B)Q\langle\sigma(v)v\rangle \quad [\mathrm{J\,m^{-3}\,s^{-1}}]. \tag{19}$$

and the rate of energy generation per unit mass is then

$$\epsilon = \frac{n(A)n(B)}{\rho}Q\langle\sigma(v)v\rangle \quad [\mathrm{J\,kg^{-1}\,s^{-1}}]. \tag{20}$$

The total luminosity of a star may then be expressed as

$$L = \int_M \epsilon dm = \int_V \epsilon\rho dV = \int_0^R 4\pi r^2 \epsilon\rho dr \tag{21}$$

where the values of ϵ are determined by the physical conditions in the star and the nuclear reactions that can occur. We now consider which nuclear reactions actually take place in a star, and the rate of energy generation associated with them.

1.4 Hydrogen burning

During most of their lives, stars derive their energy from the fusion of hydrogen into helium, which can be written schematically as

$$4\,{}^1\mathrm{H} \rightarrow {}^4\,\mathrm{He} + 2e^+ + 2\nu_{\mathrm{e}} \tag{22}$$

where we note that this reaction conserves the total charge, baryon number and lepton number (noting that positrons are anti-particles and hence have negative lepton numbers that balance those of the emitted neutrinos). Although it is clear that the reaction does not proceed as outlined in eqn. (22), since the probability of getting four hydrogen nuclei to collide and fuse simultaneously is completely negligible, the difference in the masses of the reactants and the products allows us to use the mass-energy equivalence to determine that the energy released by converting 4 hydrogen nuclei to a helium nucleus is $Q = 26.73$ MeV.

When calculating the energy generation rate, ϵ, we must subtract the neutrino energy, since neutrinos escape directly from the star. The correction to be applied, however, depends on the details of the reactions that produce the neutrinos, since the branching ratios between the different reactions depend on the conditions within the star (namely the density and temperature).

There are two basic ways in which the overall reaction (22) may be accomplished: the PP-chains, which directly convert H to He; and the CNO cycle, which involves C, N and O acting as catalysts in reactions that ultimately convert H to He.

The various branches associated with the PP-chain are shown in Fig. 4, with the indicated branching ratios being appropriate for conditions in the Sun. A colour diagram that also shows the energies associated with the PP-chain reactions is shown at the end of these lecture notes in Fig. 6. The first reaction is the collision of two protons, leading to the formation of a deuterium nucleus. Although this reaction has the smallest Coulomb barrier, it is the slowest of all in the PP-chain because it involves a beta decay of a proton to a neutron that involves the weak interaction. Hence, this reaction controls the combined rate of energy generation of the PP-chains. The remaining reactions are in equilibrium, in the sense that equal amounts of ^{2}H and ^{3}He are produced and destroyed.

After the formation of ^{3}He, the PP-chain can proceed in three branches. The branching ratios between the different parts of the PP-chain depend on the temperature. In the Solar core, the PP-I chain dominates, and the PP-III chain makes a very small contribution to the energy generation rate. On the other hand, the PP-III chain is very important for attempts to detect solar neutrinos: due to their high energies the neutrinos from this chain dominate measurement in ^{37}Cl detectors, and only the PP-III neutrinos can be seen by the detectors based on neutrino scattering in water. The strong temperature dependence of the branching ratios makes the detection of these neutrinos a key test for the central temperature of the Sun.

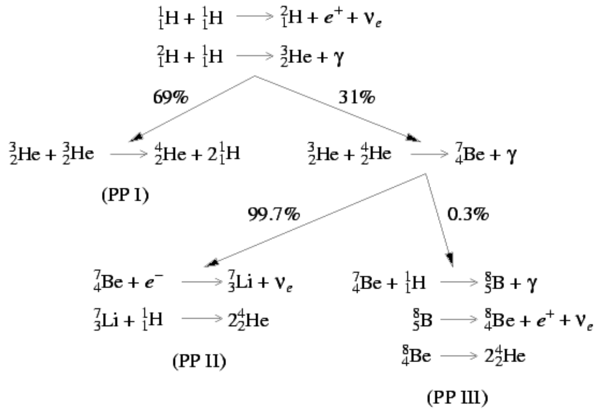

Figure 4: Schematic of the PP-chains.

The energy generation rate per unit mass from the PP-chain can be expressed as

$$\epsilon_{\rm pp} = 2.6 \times 10^{-37} X^2 \rho T^{4.5} \ \ {\rm J\,s^{-1}\,kg^{-1}} \tag{23}$$

where X is the hydrogen mass fraction. This can be written more generally as

$$\epsilon_{\rm pp} = \epsilon_{\rm pp0} X^2 \rho T^{\alpha} \ \ 3.5 \leq \alpha \leq 6 \tag{24}$$

for some constant value of $\epsilon_{\rm pp0}$.

Using eqns. (21) and (24), and assuming the hydrogen abundance is constant in the stellar interior, the total luminosity can be estimated as

$$L = 4\pi \epsilon_{\rm pp0} X^2 \int_0^R T^{\alpha} \rho^2 r^2 dr. \tag{25}$$

When the star is approximated by a polytrope of index n, we have $\rho = \rho_{\rm c}\theta^n$, $T = T_{\rm c}\theta$ and $r = (R/\xi_1)\xi$, and hence

$$L = 4\pi \epsilon_{\rm pp0} X^2 T_{\rm c}^{\alpha} \rho_{\rm c}^2 \left(\frac{R}{\epsilon_1}\right)^3 \int_0^{\epsilon_1} \theta^{2n+\alpha} \xi^2 d\xi. \tag{26}$$

With $T_{\rm c} = b_n G M \mu m_{\rm H}/(k_{\rm B} R)$ and $\rho_{\rm c} = a_n 3M/(4\pi R^3$, as presented in week 4, we obtain the simple scaling relation

$$L = A_n X^2 \mu^{\alpha} \frac{M^{2+\alpha}}{R^{3+\alpha}} \tag{27}$$

where μ is the mean molecular weight and A_n depends on the polytropic index n only.

The CNO cycle operates in stars that contain C, N and O, and proceeds as shown in Fig. 5. The reactions start with ^{12}C and proceed through a sequence of proton captures, interrupted by positron (beta) decay with emission of neutrinos; ^{12}C is produced at the end of the sequence and hence acts as a catalyst. The conversion of ^{14}N to ^{15}O has the smallest probability of all the reactions in the cycle; hence, once the cycle operates in equilibrium this reaction determines the overall reaction rate.

An estimate of the energy generation rate per unit mass by the CNO cycle, appropriate for typical stellar conditions, is given by

$$\epsilon_{\rm CNO} = 7.9 \times 10^{-118} X Z \rho T^{16} \ \ {\rm J\,s^{-1}\,kg^{-1}} \tag{28}$$

where we have assumed that that the total abundance of CNO elements is a fixed fraction of the heavy element abundance, Z. A more general expression is

$$\epsilon_{\rm CNO} = \epsilon_1 X Z \rho T^{\beta} \ \ 12 \leq \beta \leq 20. \tag{29}$$

We see that the energy generation rate from the CNO cycle has a much greater sensitivity to the temperature than the PP-chain. Hence, the PP-chains dominate at relatively low temperatures and the CNO cycle dominates at higher temperatures. Given how our estimates for the central temperature in the lectures from weeks 3 and 4 scale with the stellar mass, we expect the CNO cycle to dominate hydrogen burning in massive stars.

$$
\begin{array}{ccc}
{}^{12}C + {}^{1}H & \rightarrow & {}^{13}N + \gamma \\
{}^{13}N & \rightarrow & {}^{13}C + e^{+} + \nu_e \\
{}^{13}C + {}^{1}H & \rightarrow & {}^{14}N + \gamma \\
{}^{14}N + {}^{1}H & \rightarrow & {}^{15}O + \gamma \\
{}^{15}O & \rightarrow & {}^{15}N + e^{+} + \nu_e \\
{}^{15}N + {}^{1}H & \rightarrow & {}^{12}C + {}^{4}He
\end{array}
$$

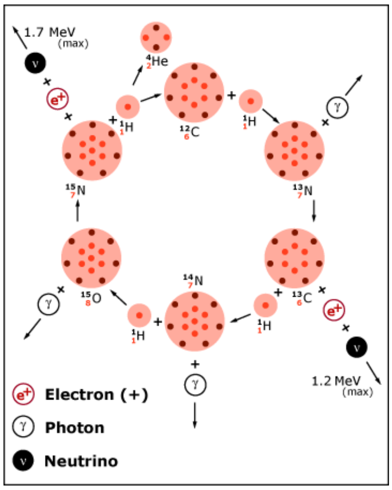

Figure 5: Schematic diagram of the CNO cycle.

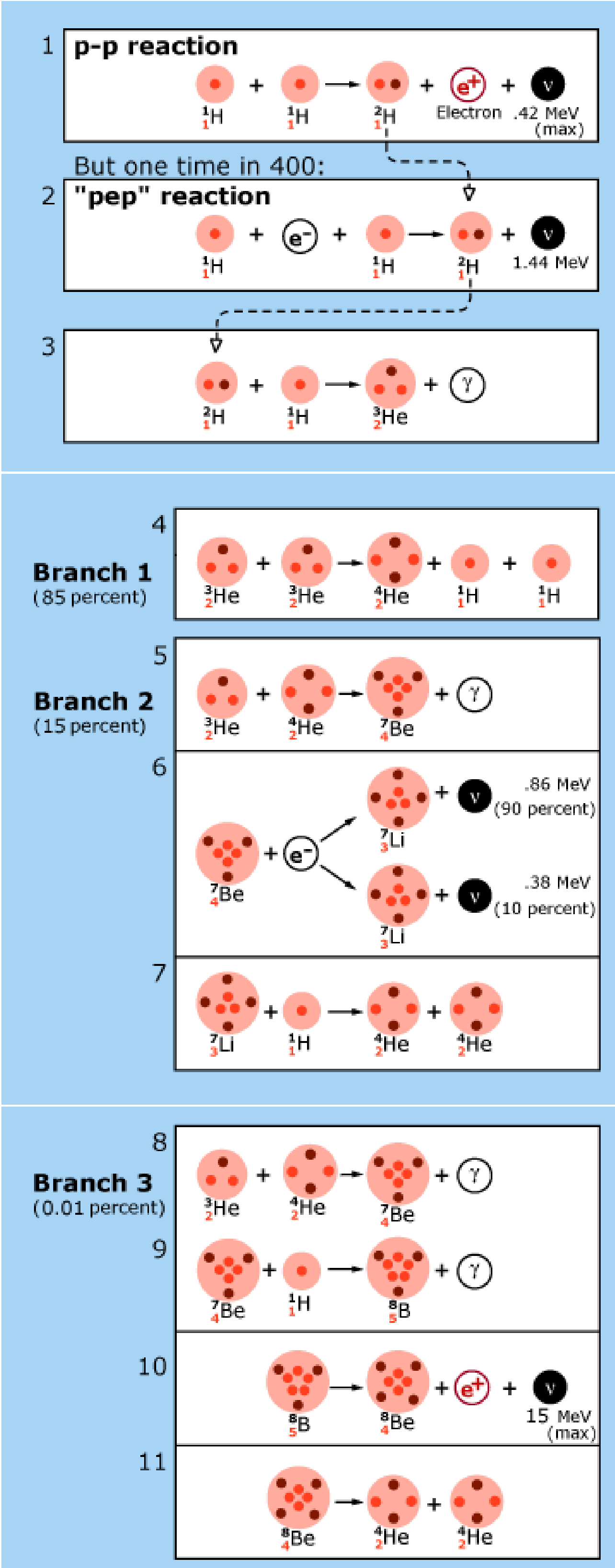

Figure 6: Schematic diagram of the PP-chains.